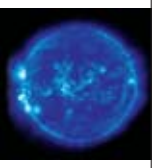

**Inertial-confinement fusion is an avenue of research that is being explored to achieve the fusion of light elements, concurrently with magnetic-confinement fusion**. Whereas, in the latter, confinement holds the plasma at a very low density ($10^{-5}$ times atmospheric density) over time spans of the order of a second, the "inertial" approach consists in achieving much higher densities ($10^{6}$ times atmospheric density), sustained over time spans determined by the system's inertia (typically, a few tens of picoseconds). Lasers allow a very high energy concentration within the time spans required for inertial-confinement fusion. The Megajoule Laser (LMJ: Laser Mégajoule) being built by CEA for defense applications should thus enable inertial-confinement ignition and burn to be achieved, by the beginning of the next decade. The temperature and pressure conditions it will make possible to achieve will also enable investigation of thermonuclear phenomena in stellar-type plasmas.

# Inertial-confinement fusion

## Principles of inertial-confinement fusion: compression and brevity

The process of inertial-confinement fusion may be likened to that of a Diesel engine: compression of the fuel mix – brought to a density 1,000 times greater than that of the solid or liquid state – results in ignition and explosion, inside a time interval shorter than a hundred picoseconds.

Whichever technology is adopted, the problem set for nuclear **fusion** remains the same: to overcome the repulsion of two **light-element nuclei**, so these may pool their **nucleons**, to form a heavier element. The nuclear-fusion reaction least difficult to achieve is that which can occur with **deuterium** (D) and **tritium** (T), two **isotopes** of **hydrogen**. This gives birth to a **helium**-4 nucleus (**alpha particle**), having an energy of 3.52 **MeV**, and a 14.06-MeV **neutron**. The considerable energy that must be imparted to the two

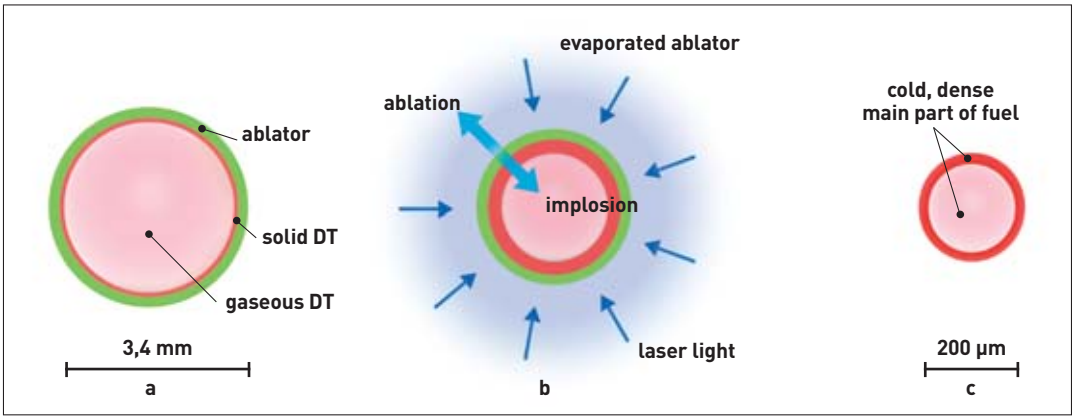


Figure 1.
In its initial state (a), the target designed for ignition with LMJ (here in a direct drive scheme) comprises a shell of DT ice, at a temperature of 17 K, covered by an ablator, made of plastic material or solid DT. DT at saturated-vapor pressure fills the central part. When illuminated by the laser (b), the heated material is ejected outward by ablation, this inducing, by return reaction, a thrust compressing the target.
At the point when ignition occurs, target radius is one-fifteenth of the initial radius (c). The ablator has evaporated away, and the fuel mass is essentially contained inside a very dense shell (200–500 g/cm$^3$). Thermonuclear reactions are initially set off in the central region, which is less dense but extremely hot (about 100 million degrees).

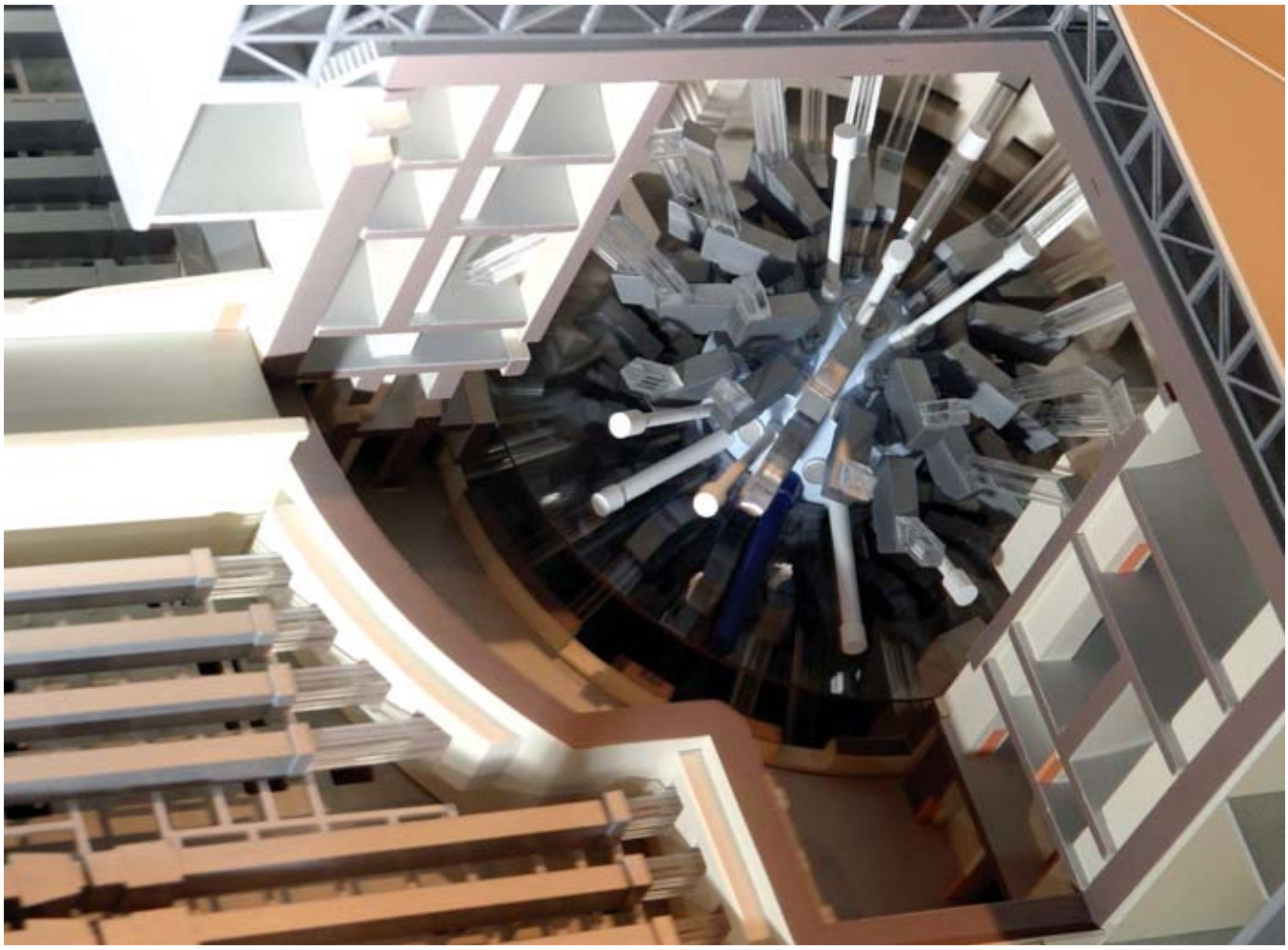

G. Rolle/REA/CEA

Mockup of the Megajoule laser currently being built by CEA at the Aquitaine Scientific and Technical Research Center (CESTA), at Le Barp near Bordeaux. At left, part of the laser lines. At right, the experiment chamber (in blue) onto which all laser lines converge, and numerous diagnostic equipement items (white).

deuterium and tritium nuclei, in the form of relative velocity, is supplied by thermal agitation. Maximum probability of occurrence for this fusion reaction, in a DT **plasma**, arises at around 70 **keV**. Probability reaches one tenth of this value at around 10 keV.

A classic criterion for plasma fusion is the *Lawson criterion*: this corresponds to ensuring that the fusion energy released (weighed by an extraction efficiency of 30%) is greater than the energy that must be supplied to the plasma to bring it to burn conditions. Now the fusion energy released per unit volume is dependent on three parameters: temperature, density (i.e., "number density": the number $n$ of **ions** per unit volume), and the time $\tau$ during which these two conditions are sustained. Bearing in mind fusion reactions occur effectively from 10 keV on, the Lawson criterion for a DT plasma takes the form: $n{\cdot}\tau > 2{\cdot}10^{14}$ ($m^{-3}s$).

Magnetic-confinement fusion meets this criterion by maintaining densities greater than $10^{14}$ ions per cubic centimeter over durations well above one second. In **inertial-confinement** fusion, the approach is completely different: plasma is very heavily compressed, up to densities of $10^{26}$ ions/$cm^3$ (i.e. 300 g/$cm^3$!), however such densities are only sustained for a very short duration (some $10^{-11}$ s) before the plasma expands (explosion).

For a large enough proportion of the **fuel** to be burnt, the fusion process must be more rapid than the fuel's expansion under its own internal pressure. This condition will be met if the fuel is sufficiently hot and dense, or, more accurately, concentrated (the product $\rho \cdot R$ of mass density by the radius of the fuel sphere characterizes this property). In the case of a spherical microtarget containing a deuterium–tritium (DT) mix at a temperature of 40 keV, for instance, it will be possible to burn one third of the fuel once the product $\rho \cdot R$ gets over 3 g/$cm^2$. For a DT mass $M$, this criterion further takes the form:

$$\rho_{(g/cc)} \geq \frac{10}{\sqrt{M_{(g)}}} :$$

the smaller the mass of fuel to be burnt, the higher the density required, and hence the greater the mix compression needed.

Bearing in mind the specific energy of DT fusion (340 MJ/mg), it will for instance be possible to achieve a yield of 100 MJ with 1 mg DT, if mix density reaches some 300 g/$cm^3$ (i.e. over 1,000 times the solid density) for a temperature of 40 keV. Sphere radius will then be 100 **micrometers**, and time allowed for burning (*confinement time*) about 25 **picoseconds**.

Such experimental conditions may be achieved, in theory, through implosion of a spherical shell of solid, **cryogenic** fuel (see Figure 1), by means of a laser delivering energy of 1–2 megajoules (1–2 MJ). To achieve such an outcome, a number of parameters have to be

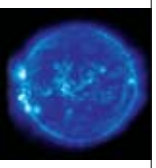

mastered, as will now be set out using the selfsame example, of a 1-mg DT mix contained in a microtarget.

### Hot-spot ignition

First, the energy imparted by the laser to the DT mix itself must be kept to a minimum. Compression requires relatively little energy: about 15–40 kJ per milligram, if this is efficiently carried out. On the other hand, achieving the *temperature* required to initiate burning would call for much greater energy: 1.1 MJ per milligram. To reduce this constraint, only a small part of the fuel mass (10–20 μg) is brought to ignition temperature. This high-temperature "spark," known as a *hot spot*, confined by the remaining, very dense fuel surrounding it, will be able to initiate self-sustained burn, provided it can "recapture" a sizeable portion of the fusion energy released, essentially that carried by the alpha particles emitted.

### Fuel compression

In such conditions, overall compression and hot-spot heating energy amounts to about 60 kJ. This energy must be imparted to the fuel, initially, primarily in the guise of kinetic energy: the required implosion velocity, of the order of 400 km/s, entails a pressure close to 100 **megabars** (Mbar), i.e. $10 \cdot 10^{12}$ pascals. Such pressure and velocity can be achieved by means of a power laser and a suitable target, consisting in a shell comprising an outer plastics layer and an inner DT layer, this taking the form of ice (see *Cryogenic microtargets, key components of the inertial-confinement experiments with LMJ*). When an intense laser beam interacts with a target, indeed, a plasma forms on the surface through **ablation**, this then being ejected outward at high velocity. By reaction in return, centripetal momentum (if the target is spherical) is transferred to the part that is still cold, a process which may be termed, by analogy, a *rocket effect*. The pressure generated is at a maximum close to the ablation front. This is linked to laser intensity and wavelength, through a scaling law: $P_{(\mathrm{Mbar})} = 40\ (I_{(\mathrm{PW/cm^2})} / \lambda_{(\mu\mathrm{m})})^{2/3}$. This law states that short wavelengths are more effective, for a given illumination, in terms of inducing high pressure: a pressure of 100 megabars may be obtained with a laser having an intensity of around $10^{15}$ W/cm$^2$, at a wavelength of 0.35 μm.

The laser energy required depends on the hydrodynamic efficiency of the ablation-induced implosion. A 5% efficiency entails, for the present example, energy of 1.2 MJ. Suitable temporal shaping of the laser pulse can help optimize the compression process (see Figure 2). At the same time, other parameters have to be optimized, first of all the symmetry of illumination of the microballoon containing the DT mix.

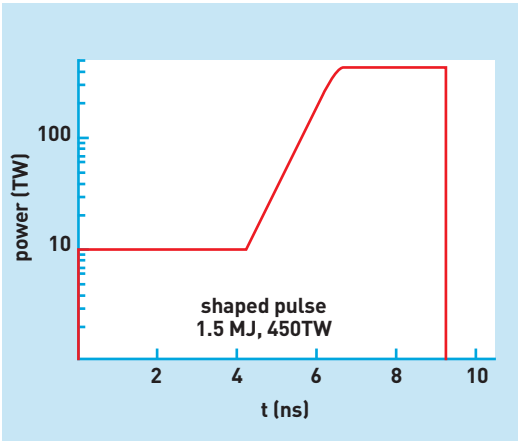


Figure 2.
During fuel compression, the pressure law is achieved through temporal shaping of the laser's power. An initial intensity level at 10 terawatts for 4 nanoseconds (ns) causes an initial shock, of 8 megabars. This is followed by a gentle slope, leading to the main pulse, ending at 9.2 ns. The laser is stopped, and the shell continues with its motion right down to final compression, which is achieved around 10 ns.

### Perfect illumination symmetry

Indeed, the example just considered implies perfect spherical symmetry of the sample and the illumination it receives, since any departure from sphericity will impair compression effectiveness, to the extent it may prevent onset of the hot spot.

The laser used will thus have to feature a large number of beams, to ensure the best possible illumination symmetry. In practice, errors in pointing, sample positioning, and balancing of overall illumination are unavoidable. Stringent technical specifications, including for instance pointing uncertainty of less than 50 micrometers, have been drawn up by CEA specialists, to keep illumination nonuniformity under 1%, which allows the specific conditions for **ignition** to be achieved.

### Countering hydrodynamic instabilities

Other processes may also preclude fusion conditions from being achieved: hydrodynamic instabilities. The ablative implosion described earlier consists in accelerating a dense medium by means of a less dense medium (see Figure 3). This situation is analogous to that of a heavy fluid lying above a lighter fluid in a gravity field. Such a configuration is inherently unstable (Rayleigh–Taylor instability), and any flow perturbation, relative to the ideal spherical shape, is amplified over time. Growth initially is exponential; then, as soon as the fault's amplitude becomes comparable in size to its wavelength, nonlinear saturation of its growth sets in. It should be pointed out, finally, that the ablation process, which is the cause of the motion, tends to mitigate its unstable character.

Initial perturbations arise owing to surface roughness of the interfaces between the media, and illumination nonuniformity. To keep them to a minimum, targets will have to feature mean outside roughness of 50 **nanometers**, and inside roughness (DT ice) of 1 micrometer.

### Laser–plasma interaction instabilities

Other types of instability may also perturb fusion experiments. These are instabilities related to laser–plasma interaction. Indeed, as we have seen, from the outset of illumination, a plasma forms through ablation. Throughout illumination, this plasma will interact with the laser wave, and may thus absorb it. For moderate laser intensities, absorption rate ranges from 60% to total absorption, according to the material undergoing irradiation. At high intensities (greater than $10^{15}$ W/cm$^2$, for a wavelength of 0.35 μm), plasma instabilities may occur.

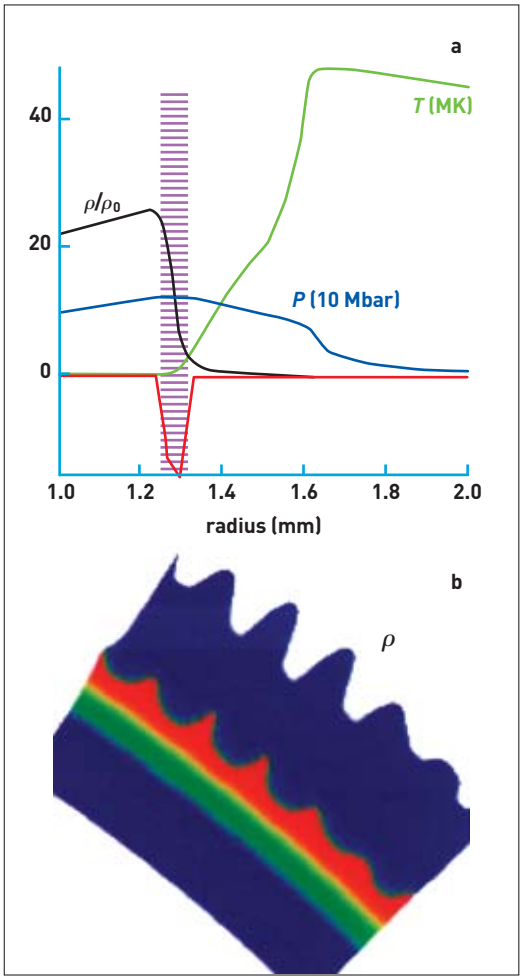


Figure 3.
Shown at (a), the thermodynamic state of the ablation front at the time when shell acceleration occurs. In the hatched region, the product of the density r and pressure P gradients is negative: this region is subject to Rayleigh–Taylor instability. At (b), a representation of the density modulation obtained in numerical simulation of an implosion, taking into account laser signature. Nonlinear development of instability may be observed.

*Ponderomotive filamentation* instability, for instance, is triggered through a combination of (temporal or spatial) over-intensities in the illumination profile and local fluctuations in the plasma's refractive index. This results in self-focusing of the laser wave: light focuses into tiny filaments, detrimental to illumination uniformity.
Further, the plasma, being a compressible, conducting medium, supports ion acoustic waves and electron waves. In some conditions, these waves may exchange energy with the laser wave, and undergo resonant coupling. This results in back-scattering of part of the laser energy (*stimulated Raman back-scattering* and *stimulated Brillouin back-scattering*), together with production of high-energy **electrons**, liable to preheat the fuel prior to compression.
Since such instability processes are detrimental to laser-energy absorption by the target, many theoretical and experimental investigations focus on them. The outcome of this work has been the design of targets that are robust with respect to the onset of such instabilities, and development of appropriate techniques to prevent the occurrence of laser over-intensities (*smoothing*).

## Direct or indirect drive?

In the aforegoing description, consideration was given to direct interaction between the laser wave and the microballoon containing the DT fuel: this is the so-called *direct-drive* scheme (see Figure 4a). Another scheme is available, affording a number of benefits, but equally some drawbacks: this is the so-called *indirect-drive* scheme (see Figure 4b). This consists in directing the laser beams onto the inside walls of a gold vessel (the *cavity*, or *hohlraum*), to generate **X-radiation** inside it. At the center of the cavity, the microballoon containing the DT fuel is put in position. The X-radiation generated is confined inside the hohlraum as in an oven, and ultimately arrives close to black-body radiation at 300 eV (i.e. 3.5 million **kelvins**). This has the ability, just as direct laser radiation, to cause the ablative implosion of a spherical microballoon, with, in this case, better illumination uniformity and enhanced hydrodynamic efficiency. It also induces higher ablation speed, appreciably restricting growth of hydrodynamic instabilities. Physicists at CEA's Military Applications Division consider this scheme to be the surest way of achieving thermonuclear fusion with gains greater than unity. While it is well suited to an experimental utilization, in particular in the context of the Simulation Program, its low efficiency (in terms of energy transferred to the fuel) means it is hardly appropriate for future laser-driven energy generation. It could become competitive through the use of other generators, such as heavy-ion beams.

## Experimental and simulation results

Laser-driven inertial-confinement fusion nowadays – particularly over the past decade – has the benefit of a very large body of established experimental results. Direct drive was mainly investigated in the United

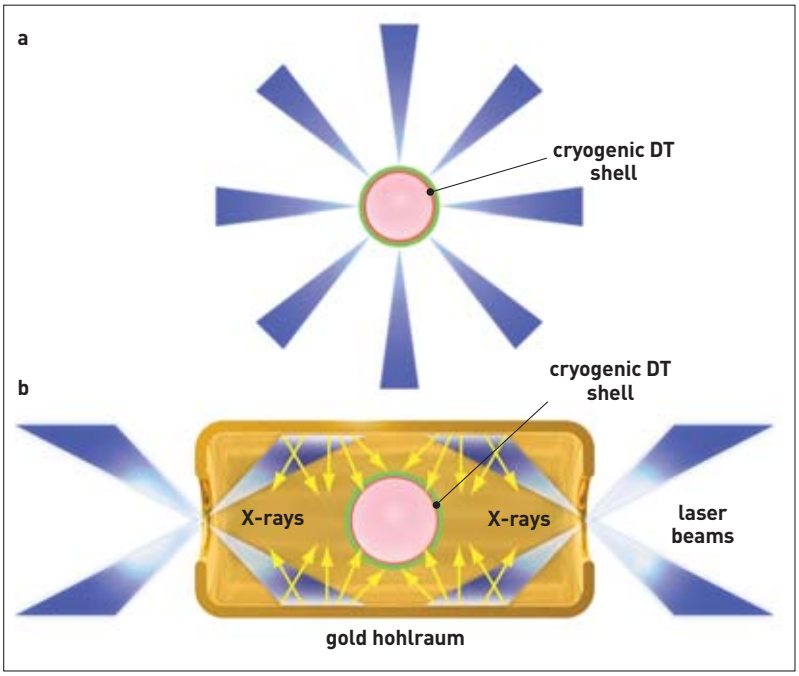


Figure 4.
Schematics of direct (a) and indirect (b) drive. In the first case, laser beams interact directly with the target. In the second, they interact with the walls of the cylindrical hohlraum holding the microballoon. The walls emit X-radiation, this interacting in turn with the microballoon.

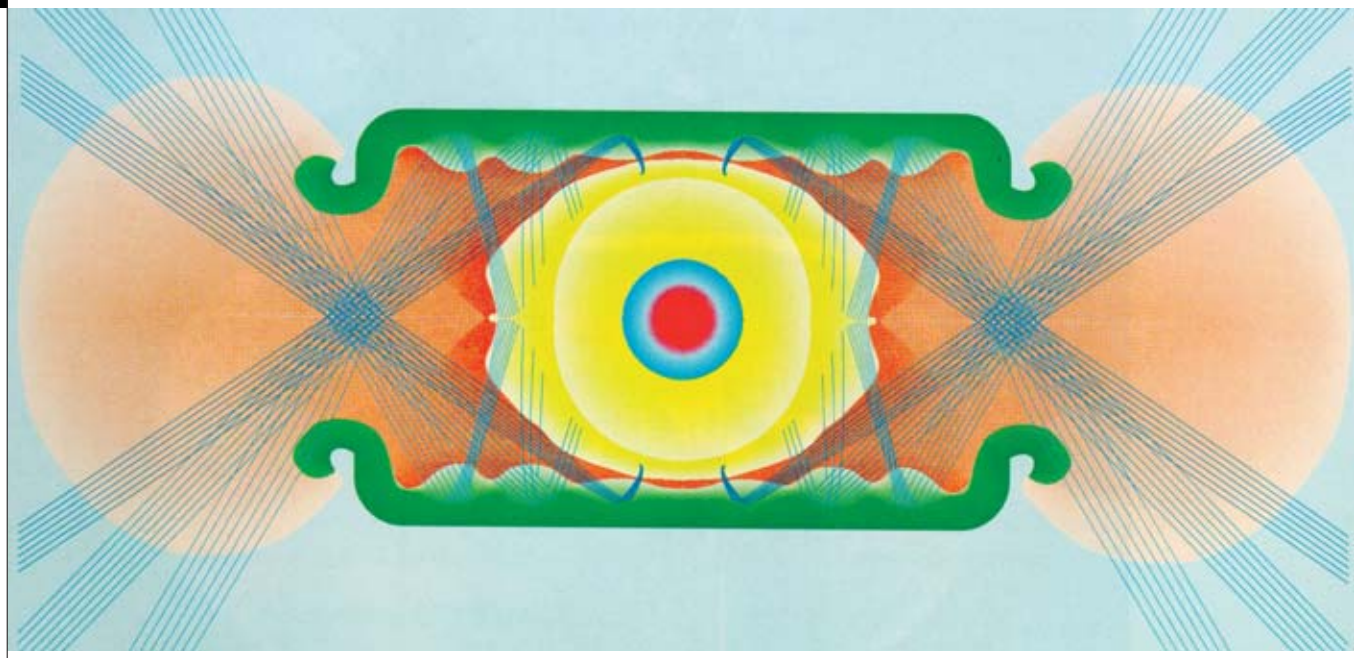

(From a graph by F. Thiais.)

Figure 5.
Simulation of a microballoon implosion inside an indirect-drive hohlraum, described by a two-dimensional Lagrangian mesh (end of the implosion). This type of simulation has enabled experiments on hohlraum-irradiation symmetry to be reproduced.

States, at the University of Rochester, which currently runs the Omega laser (60 beams, delivering 40 kJ on target), and in Japan, at Osaka University, running the Gekko XII laser (12 beams, 15 kJ delivered on target). Indirect drive has also been extensively investigated in the United States, drawing on the facilities at the Lawrence Livermore National Laboratory (in particular the Nova laser, featuring 10 × 3-kJ beams), and in France, with CEA's Phébus laser (2 × 3-kJ beams), based at Limeil (near Paris).
All these experimental investigations have enabled the reproduction, and a better understanding, of the many processes involved in inertial-confinement fusion, be it through adoption of one or the other drive scheme: laser–plasma interaction, laser or X-ray ablation, **thermalization** of radiation inside the hohlraum, implosion, etc.

NIF/LLNL

The experiment chamber in the US National Ignition Facility (NIF), which is the equivalent of the French Megajoule Laser.

These processes, however, or a number of them, at least, can only be experimented on, at the appropriate scale for fusion to be achieved, in a laser facility affording adequate performance, in terms of energy, power, and precision. World-wide, two such facilities are currently being built: the Megajoule Laser (LMJ: Laser Mégajoule), in France, at CEA's Aquitaine Scientific and Technical Research Center (CESTA: Centre d'études scientifiques et techniques d'Aquitaine); and NIF (National Ignition Facility), in the United States, at the Lawrence Livermore Laboratory.
Concurrently with laser experimentation, numerical simulation allows analysis, by computation, of the functioning of the future targets that will enable inertial-confinement fusion to be achieved. Such simulation is based on mathematical **modeling** of the physical processes involved. These models are then expressed in the form of algorithms, which are coupled and brought together in large computational "**codes**." The Ile de France (Paris region) Center of CEA's Military Applications Division (at Bruyères-le-Châtel) has expertise in the simulation of complex systems, of many years' standing now, supported by the computation capacity of the Tera machine (5 **teraflops** peak), installed in the context of the Simulation Program. With such resources, physicists from that laboratory are carrying out simulations of inertial-confinement experiments in two or three spatial dimensions (see Figure 5). These simulations are integrated simulations, insofar as they take into account all of the mechanisms that come into play in the targets, from laser–plasma interaction to fuel thermonuclear yield.

## What would an inertial-confinement fusion reactor be like?

Beyond the essential step of achieving ignition, there is also a call to consider what a useable, economically via-

ble reactor would be like, and to provide answers to some key questions: generating 1 GW of electrical power will require a laser with the capacity to deliver, every second, ten pulses of 5 MJ each, with an overall efficiency, as regards electrical power consumption, better than 10%. The energy of the 14-MeV **neutrons** generated must be converted into electrical power with an efficiency better than 30%. Finally, on the basis of present costs per gigawatt–hour, DT samples will have to be produced at a cost of less than 1 euro apiece. Major technological challenges will thus have to be taken up.

The first laser-driven thermonuclear neutrons were obtained, at the end of the 1960s, by CEA teams at the Limeil–Valenton Research Center. Nearly fifty years on, the plan is to achieve implosions where, for the first time, the thermonuclear energy generated will be greater than the laser energy supplied. Such an outcome will open the way to studies for the development of an inertial-confinement fusion reactor.

# The Megajoule Laser: instrument *par excellence*

The physics of laser-driven inertial-confinement fusion dictates the main characteristics of the Megajoule Laser (LMJ: Laser Mégajoule), currently being built on CEA's CESTA site, near Bordeaux. Many technological challenges have had to be taken up.

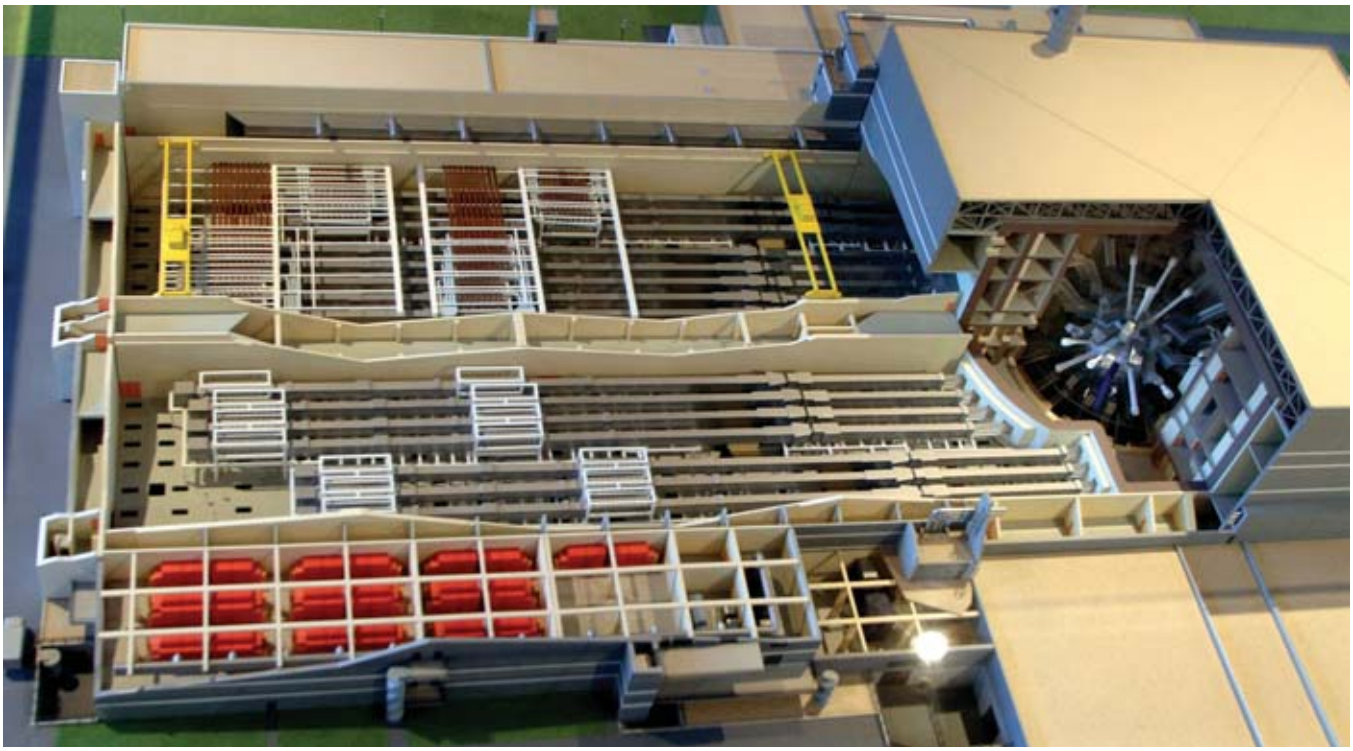

G. Rolle/CEA

Mockup, showing siting and layout of the experiment chamber and distribution of the laser lines in the LMJ building.

As described above, the process whereby laser-driven **fusion** of a **DT** microtarget is achieved entails characteristics, for the laser, that are dictated by the physics of fusion. It is thus necessary to have access to energy of the order of 1.8 **megajoule** and power of several hundred **terawatts** (TW), at a wavelength of 351 **nanometers**. Further, to ensure homogeneous illumination of the target, pointing accuracy, for the laser beams, must be better than 50 **micrometers** (50 μm). All of which characteristics must be taken on board for LMJ operation (see Box).

## Material for the laser: a crucial choice

The experience accumulated at CEA through operation of the Phébus and Octal high-power lasers naturally commanded the choice of material for the laser, to deliver the energy required: phosphate glass, doped with neodymium $Nd^{3+}$ **ions**. This is the only material that can be produced in large quantities, with the required quality, capable of delivering the desired laser energy. The $Nd^{3+}$ ion, brought to an excited electronic state, emits laser light at a frequency of 1,053 nm, which, by frequency conversion, allows the sought-for 351-nm wavelength to be achieved.

The amount of laser energy that may be extracted per unit volume of $Nd^{3+}$:glass material (a few joules per liter) dictates the size of the optical components, fabrication of which has to be mastered, as must their operational qualification and utilization. Moreover, laser-flux resistance of such parts is limited to a few joules per square centimeter. Beyond this value, they

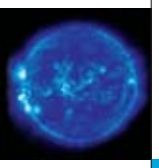

## A few orders of magnitude

| | |
|---|---|
| **1.8 megajoule (MJ)** | 0.5 kilowatt–hour (kWh): consumption of a television set over one evening |
| **500 terawatts (TW)** | 500,000 nuclear power stations connected in parallel |
| **100 megabars (Mbar)** | 100 million atmospheres |
| **10 nanoseconds (ns): duration of the laser pulse and of the microballoon implosion** | time taken by light to travel 3 meters |
| **400 kilometers per second (km/s)** | covering the distance from Paris to Marseilles in 2 seconds |
| **1 teraflops (Tflop)** | 1,000 billion floating-point multiplications per second (one simulation may last tens of hours!) |

undergo damage, or destruction. Dimensions of the laser beam, for a given energy, must be set accordingly.
It is through consideration of these technological constraints, and the physical conditions entailed by the **inertial-confinement** fusion mechanism that the design of the LMJ laser was arrived at. It comprises an ensemble of 240 laser beams, each delivering an energy of 7.5 kJ at 351 nm. This energy is uniformly distributed over a beam of square section (40 × 40 cm).

### Two hundred and forty beams to illuminate the microtarget

To simplify concurrent management of the 240 beams, which must have the same energy and arrive at the same time (within less than 15 **picoseconds**) on the sample, they are transported and focused onto the target in groups of four (quadruplets).
In the LMJ building, these laser lines are distributed over four halls, lying on either side of the experiment chamber where the microtarget is sited. To ensure stability of the whole and minimize vibrational problems, the walls of the building are uncoupled from the ground. The eight beams in each laser line are grouped into two quadruplets. Each of these quadruplets is directed onto the sample by means of transport mirrors. The two apertures (having a diameter of about 300 μm) of the cylindrical cavity holding the microtarget each allow 120 beams to pass through. To ensure illumination symmetry, the quadruplets are distributed in accordance with a conical symmetry, and grouped in packets of 10 into three cones, having different apex angles.

### How is a beam formed?

A large number of optical elements is required, to form a laser beam delivering an energy of 7.5 kJ at 351 nm, in a time of a few **nanoseconds** (see Figure 6). The various components may be grouped into three sections, fulfilling three essential functions.

#### Shaping of the laser beam

This function consists in giving the beam the desired temporal profile and spatial energy distribution. The experiments planned require highly varied temporal profiles to be provided, within a time band ranging from about a hundred picoseconds to about 25 nanoseconds. Further, energy must be uniformly distributed over a square section. Such spatial and temporal profiles are obtained by means of two fundamental components, known as the *laser source and preamplifier module (PAM)*, which together make up the laser beam "*pilot*."
The laser source is a miniature laser oscillator, delivering an energy of 1 **nanojoule**. This source uses proven optical-fiber telecommunications technologies. Its stability is the crucial point: emission wavelength is set at 1,053 nm, to within less than ± 5 **picometers**. It is at this point, at the source, that temporal shaping is effected, this being adjustable on demand, in the range from a few hundred picoseconds to 25 nanoseconds.
The pulse from the laser source is injected into the

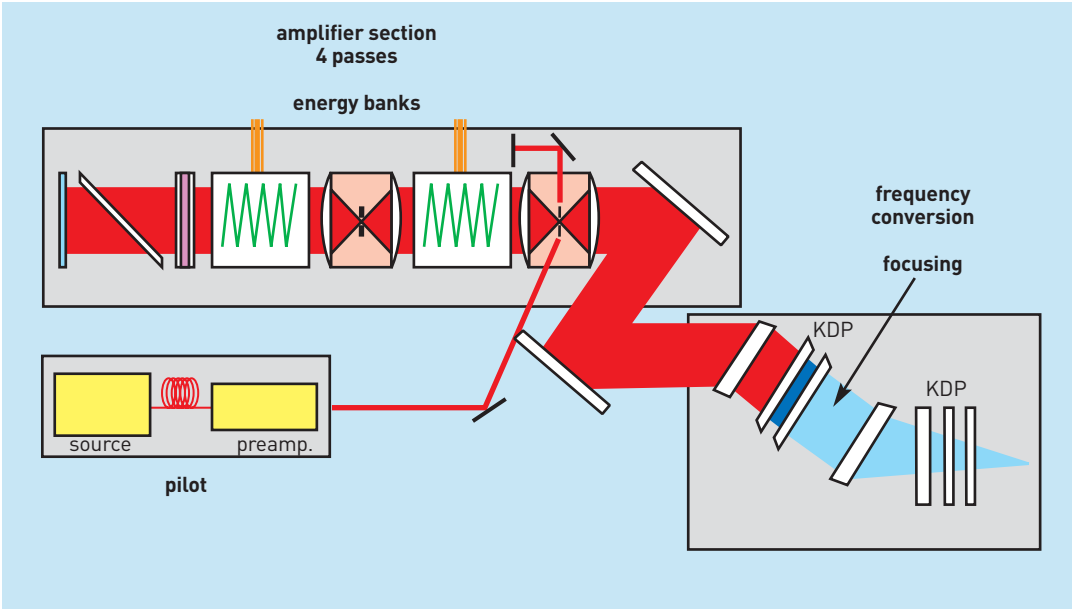


Figure 6.
Principle schematic of a laser beam in LIL and LMJ.

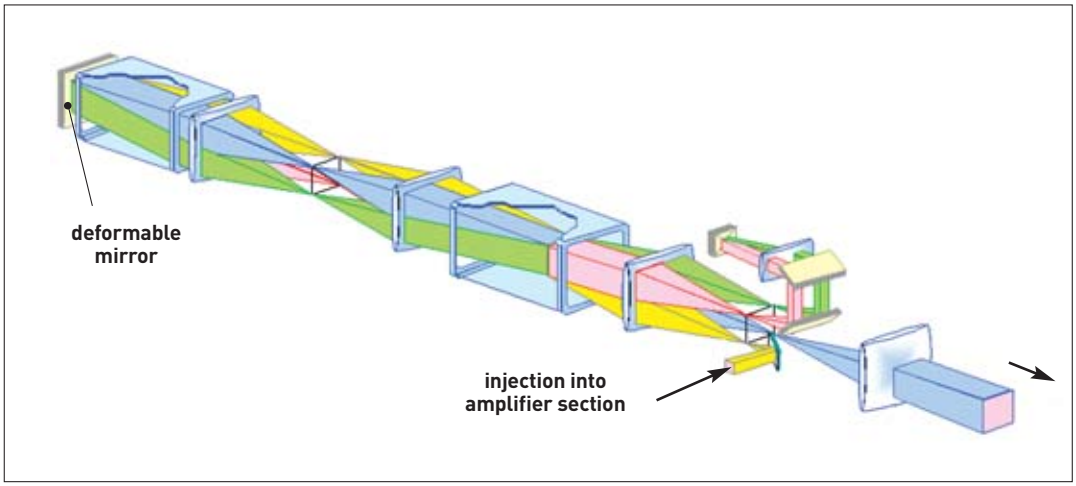


Figure 7.
Back-and-forth travel of the laser beam in the amplifier section. The different colors serve to indicate the path followed in each pass.

preamplifier module, to bring available energy up to a few hundred millijoules (i.e. an amplification factor of about $10^9$). It is in this module that energy distribution is effected and monitored, over a square, 4 × 4 cm area. An addressable optical valve (300 × 300 pixels) allows, at every point in the beam, intensity to be set so as to ensure spatial uniformity.

### Beam amplification

The amplifier section (AS) is the section into which the energy exiting the PAM is injected, to bring it up to 18 kJ. This pulse is passed four times through two sets of $Nd^{3+}$:glass amplifier plates (40 × 80 × 4 cm). These plates store light energy, supplied by flashlamps. At each pass, the beam takes up part of this energy. The energy gain, at each plate and for each pass, is 1.25. Positioned between the two sets of plates, focusing lenses, associated to a diaphragm (spatial filter pinhole), take out the parasitic (noise) beams that may arise. Beyond the two sets of plates is a reflecting mirror (M1), making the four passes possible through angular multiplexing (see Figure 7). This mirror is of the adaptive kind: its surface is deformable (being controlled by piezoelectric actuators), allowing possible beam wavefront distortions to be corrected.
One original feature, for the LMJ's laser beams, is the ability to effect all four passes through one and the same amplifier plate (see Figure 7). This allows a reduction in the number of plates required, while enhancing overall laser efficiency by extracting a maximum amount of the energy stored in the plates, and making for a smaller building size, by folding the beam's optical path back on itself.

### Frequency conversion and beam focusing

Frequency change is effected by means of KDP (potassium dihydrogen phosphate) crystals. These birefringent crystals have the property, as soon as laser intensity reaches a high value (so-called nonlinear regime), of allowing, with a strong probability, pairs of **photons** to fuse together, adding their energy to give birth to a single photon having an energy equal to the sum of their energies. Two crystals are required. The first crystal doubles beam frequency, to 526.5 nm, with about 50% efficiency. By causing the residual


G. Rolle/REA/CEA

The LIL experiment chamber being fitted out. Initial experiments are scheduled during 2004.

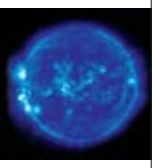

1,053-nm wave to interact with the 526.5-nm wave in a second crystal, a wave of triple frequency, at 351 nm, is obtained, with an efficiency of about 60%. The three (1,053-nm, 526.5-nm, and 351-nm) waves then travel together. They must be spatially separated, to ensure only the 351-nm wave reaches the sample. A diffraction grating is used to carry out this function. Of the holographic type, this grating is designed to effect both spectral separation and focusing of the laser beam onto the sample. This characteristic, obviating use of a focusing lens, and allowing a reduction in the number of optical components liable to be damaged, is one of the original features in the LMJ laser.

### The experiment chamber

The microtarget to be investigated will be positioned at the center of a spherical experiment chamber, kept in a vacuum. Enclosed by a 10-cm thick wall, clad with a 40-cm thickness of **neutron-absorber** concrete, the chamber, having a diameter of 10 meters and weighing 90 tonnes, will be housed in a 50-m high building (35 m above ground) that could hold the Paris Arc de Triomphe. Windows transparent to 351-nm radiation, set along the meridians, allow beam entry. Around the chamber, the diagnostic devices will be set up, charged with measuring and transmitting to an IT system the experimental data obtained. The target will have to be positioned at the center of the chamber with an accuracy of ± 5 μm, and held at below 20 K, with thermal stability better than a thousandth of a kelvin. This is undoubtedly a technological challenge to be met by the LMJ laser, as it will achieve such accuracy over a building some 300 meters long, and at the end of an optical path, for the 240 laser beams, of several hundred meters!

## The Laser Integration Line as prototype

Rather than embark directly on construction of LMJ and its 240 beams, the decision was taken to build a prototype, to validate the technological options and optimize performance, in terms of cost and maintenance. Known as the Laser Integration Line (LIL), this will reproduce two of the sixty quadruplets of the LMJ laser, and will thus comprise an ensemble of eight beams. Each of the functions needed for LMJ is to be found in this prototype.
A first beam has been fully fitted out, yielding the predicted performance, and even bettering this, since, on 4 April 2003, an energy of 9 **kilojoules** was achieved at 351 nm, after frequency conversion. A fully-equipped quadruplet, in the course of 2004, will enable the first experiments to be initiated. The remaining beams will be assembled gradually.

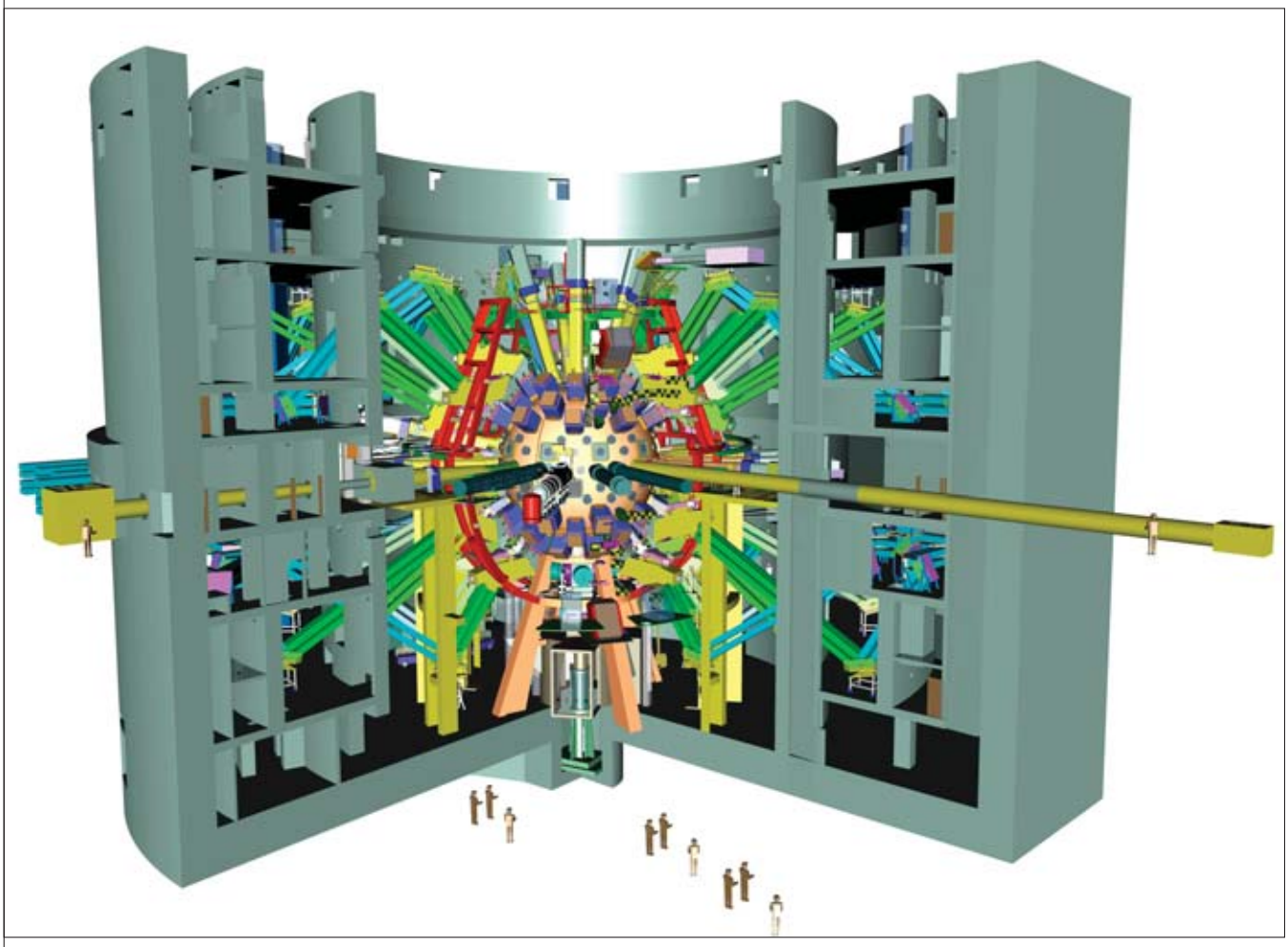

CEA/DAM

Cutaway of the building housing the LMJ experiment chamber.

# Cryogenic microtargets, key components of the inertial-confinement experiments with LMJ

There is an utter contrast between the impressive size of the LMJ's laser lines and the tiny dimensions of the inertial-confinement experiment targets, onto which they converge. These microtargets are equally high-tech concentrates.

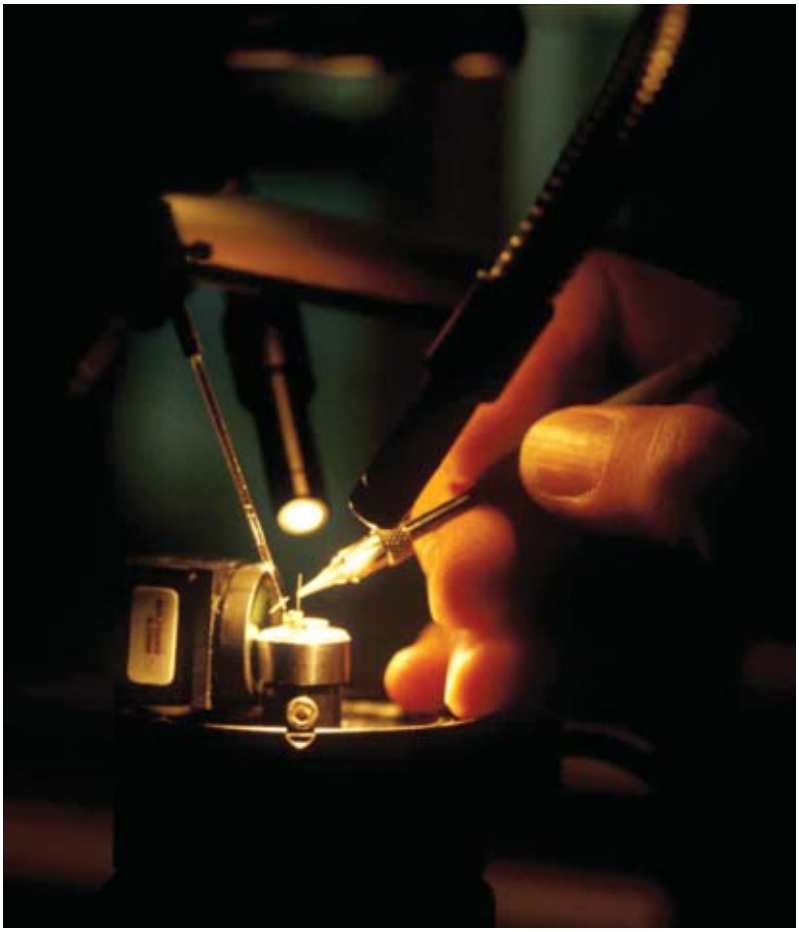

Geney-Burdin/CEA

Preparing the microtarget for an inertial-confinement fusion experiment.

The targets for the Megajoule Laser (LMJ: Laser Mégajoule) must be designed to enable bringing a very small quantity of fusile **DT** fuel to temperature and density conditions such that **thermonuclear fusion** reactions may be initiated. The fabrication process consequently takes on board the constraints associated with achieving these conditions.

In the indirect-drive irradiation scheme chosen (see Figure 8), LMJ's 240 beams will be focused on the inside wall of a cylindrical conversion cavity, or hohlraum, made from gold foil a few tens of **micrometers** thick, featuring, at either end, two apertures for the ingress of the laser beams.

Laser–matter interaction at the wall surface generates an intense **X-ray** emission, and these X-rays will compress and heat a microballoon made of amorphous hydrocarbonated (or **deuterated**) polymer, about 2 mm in diameter and 0.2 mm thick. This microballoon, held at the center of the cavity, contains the fusile DT mix, solidified at very low temperature (about 18 **kelvins**, i.e. – 255 °C).

The geometry and operational conditions thus impose stringent constraints. Manufacturing precision for the

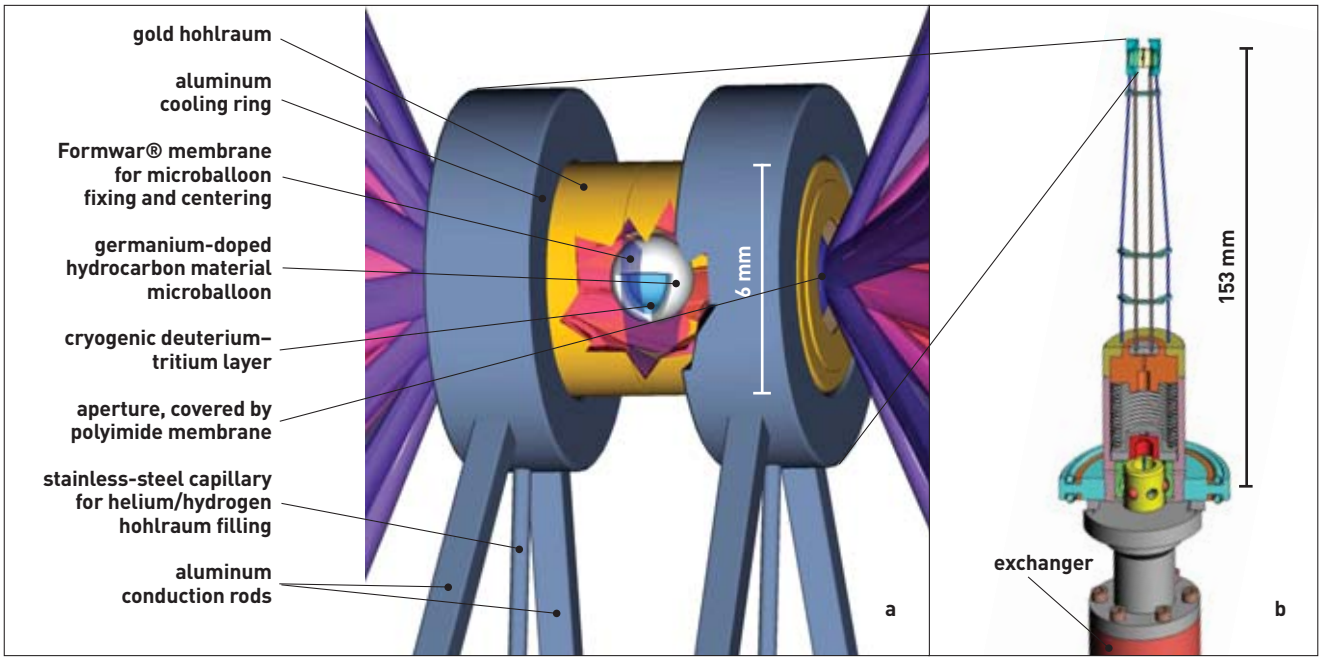


Figure 8.
Principle schematic of target functioning in indirect-drive inertial-confinement fusion. At (a), complete cryogenic hohlraum device; at (b), target assembly.

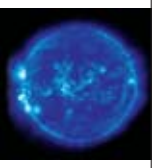

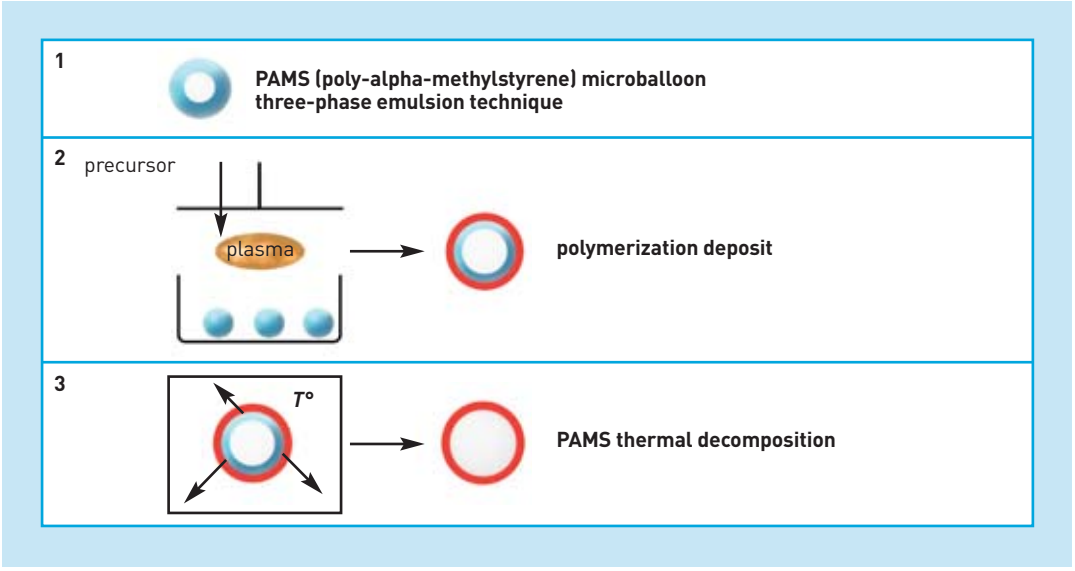


Figure 9.
Stages in the fabrication of microballoons by the "depolymerizable mandrel" technique.

various components and assemblies is equally extremely demanding, of the order of one part per thousand or per hundred thousand, according to the component. They thus entail development and implementation of very sophisticated technologies. Since 1996, research and development have achieved major breakthroughs in four main areas: the microballoon itself, the cryogenic equipment intended to fill the target capsules, the quality of the solid DT layer deposited on the inside wall of the microballoon, and the cryogenic target assembly as a whole.

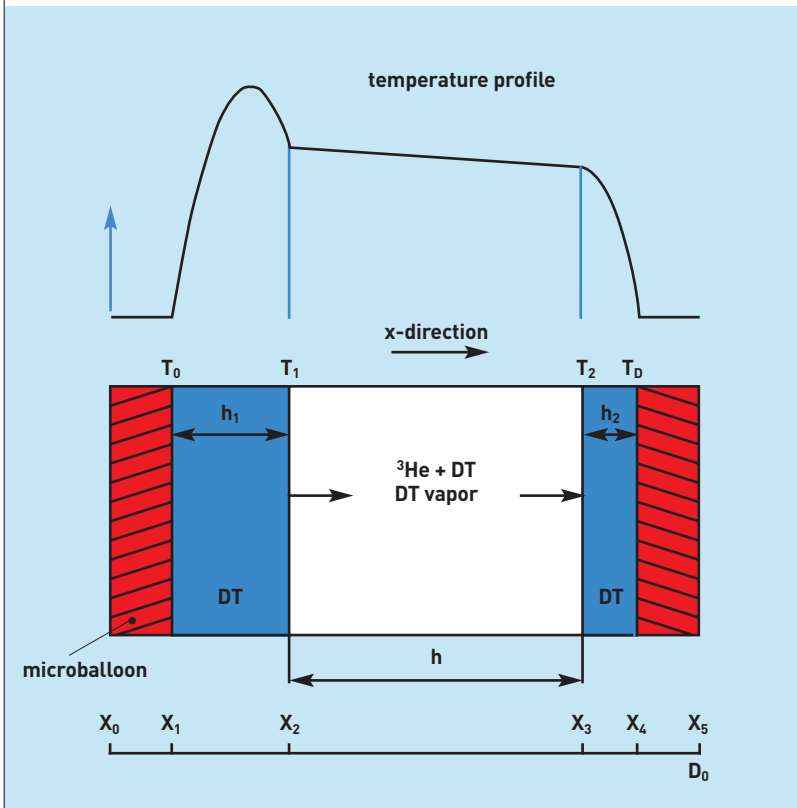


Figure 10.
Principle of natural DT redistribution.

### The $CH_x$ microballoon

The container for the fusile mix is a **hydrocarbon** ($CH_x$) microballoon, perfectly homogeneously doped with 0.4% germanium. Geometric defects are kept to less than 1 per 10,000, and roughness, both inside and outside, to less than 50 nm. To achieve such an outcome, every step of fabrication must be exactly controlled.
CHx microballoons are fabricated by means of the "depolymerizable mandrel" technique, this comprising a number of stages (see Figure 9). A spherical poly-alpha-methylstyrene (PAMS) mandrel is first made by microencapsulation techniques, using three-phase injection systems. Availability of an initial polymer (PAMS) having perfectly controlled physical–chemical properties is essential if the specifications are to be met, that the microencapsulation shaping phase aims to achieve. Onto this mandrel, a plasma-polymer deposit is made by GDP (glow-discharge polymerization), from trans-2-butene (T2B) and hydrogen ($H_2$). The initial mandrel is ultimately depolymerized by heat treatment under neutral gas. PAMS, having a decomposition temperature lower than that of the $CH_x$ plasma polymer, is taken out by **permeation** through the GDP-deposit wall. A free-standing $CH_x$ microballoon is thus obtained.
Presently, the entire technological chain has been set up. Initial studies have made it possible to fabricate objects having defects, at under 1%, that can no longer be detected by optimized optical or X-ray characterization means. High-precision characterization instruments, based on AFM (atomic force microscopy) technology, have become necessary.

### Operational cryogenic equipment to fill the targets

The polymer microballoons are filled by gas permeation at room temperature: the DT mix diffuses through the polymer wall, filling the balloon. A solid coating, 100-μm thick, must then be deposited onto the inside wall, DT solidification taking place at around 20 K. The number of **moles** of DT that will yield, once solidified at 20 K, a 100-μm DT coating corresponds to a pressure, at ambient temperature, of about 500 **bars**.

Now, the microballoons' mechanical strength is of the order of a few tens of bars. Consequently, pressure must constantly be equalized between the microballoon interior and the outside environment, to preclude the capsule exploding.
Pressure inside the filling vessel is increased gradually, to ensure there is at every point in time an equilibrium between pressures inside and outside the microballoon, up to the point where a pressure of 500 bars is reached. The required number of moles of DT inside the balloon having been obtained, temperature inside the filling vessel is then lowered, to achieve a pressure drop, and the filling vessel is gradually emptied. At DT solidification point, 19.79 K, residual pressure inside the capsule is about 200 **millibars**, corresponding to DT saturated-vapor pressure. There is now no problem for the microballoon to sustain such a pressure differential, and it can be extracted from the filling vessel. Its temperature, however, must not rise by more than about ten degrees, lest it explode. The cold chain, therefore, must not now be broken, right up to laser firing. The cryogenic target assemblies, fabricated, filled and conditioned at CEA's Valduc (Côte-d'Or *département*, eastern France), are then transported, at cryogenic temperature, to the LMJ site, in the Gironde *département* (south-western France), for experimentation.

### Conformation of the solid hydrogen-isotope coating

Once filling and freezing have been effected, the DT content drops by microgravity to the bottom of the microballoon. Redistribution must now be achieved on to the capsule's inside wall, in the form of a thin film, of precisely homogeneous thickness (see Figure 8a), to form the thin DT shell required for fusion experiments. This redistribution occurs naturally: this is the beta-layering process, using the heat generated by the tritium's **radioactive** decay. The principle may be simply explained, through a two-dimensional representation where the two opposite sides of the microballoon are figured by two parallel planes (see Figure 10). Tritium decay causes emission of an electron, this forming a volumic heat source within the solid DT. As the process is initiated, the DT coating is thicker at the bottom of the microballoon, and heat release there is thus greater. Resolution of the heat-diffusion equations shows that temperature at the solid DT–gaseous DT interface is slightly higher in this region. This difference in temperature causes a **sublimation**–recondensation process at the cold point of the solid DT. Gradually, DT deposits over the entire inside surface of the capsule through this process, provided there is strict temperature homogeneity over the capsule's outside surface, and the thermodynamic equilibrium state then corresponds to a DT coating of uniform thickness.
This natural redistribution process thus allows coatings of uniform thickness to be obtained. However, to preclude development of hydrodynamic instabilities during implosion, surface roughness of the DT coating must be kept at sub-micron scale (see above, *Countering hydrodynamic instabilities*), which is not feasible through natural redistribution. To assist nature, an additional heat flux is delivered by means of a tunable infrared laser: its wavelength is set to coincide with absorption lines of the solid DT mix, which thus absorbs the laser radiation and undergoes a rise in temperature. This additional heat allows the DT redistribution process to be amplified and controlled, and a reduction in sur-

CEA

Prototype cryogenic-target carrier (CPC) in use, as a collaboration between CEA/Grenoble (Low Temperatures Service) and CESTA (Power Lasers Department). This item, which was delivered in 2002, enabled validation of the cryogenic pincer's thermal-regulation performance. Mechanical performance (positioning accuracy and loading of a target in vacuum, in cold conditions, and in fully-automatic mode) is currently being demonstrated.

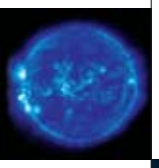

A. Gonin/CEA

Assembly rig, at CEA's CESTA Center, for the target components coming from CEA's Valduc Center being readied for LIL and the coming LMJ. Adhesive bonding is effected by hand under visual control through a binocular magnifier, and two cameras allow onscreen visualization.

face roughness to be achieved. The first coatings redistributed through infrared were recently obtained, and ongoing studies are being pursued to achieve the desired specifications.

### The cryogenic target assembly

To avoid damage to the cryogenic-target carrier (CTC) being caused by the energy released in a firing with energy gain, the cavity must be held at a distance of 100 mm from its holding collar by a lightweight structure, made from a material of low **atomic number** Z (see Figure 8a). This function is carried out by a turret, which is in turn integral with a collar enabling, in particular, connection to the cryogenic-target carrier. As regards the conversion cavity (hohlraum) assembly, the most complex and demanding aspect lies in positioning a 2.4-mm diameter microballoon at the center of a cylindrical, 6-mm diameter cavity. The hohlraum is made up of two half-cylinders over which a flexible Formwar® polymer film is stretch-formed. Drilling through the center of these films is effected by laser machining, the diameter of the openings made being smaller than that of the microballoon. The latter is then laid over the opening of one of the hohlraum parts by means of micrometric displacement and a suction holding system. The second part of the hohlraum is then placed over the microballoon, thus pressing it between the two films and fixing it into position by assembly of the two hohlraum parts. Adjustments to the diameter of the two openings and their centering allows centering of the microballoon to be effected in the *x*-, *y*- and *z*-directions. The required positioning tolerances, of ± 30 μm along all three axes, have already been achieved.

Successful outcome of these various research and development efforts, regarding sample design and fabrication, will enable the outstanding instrument that is afforded by LMJ to carry out, by the end of this decade, the long-awaited experiments on DT ignition by inertial-confinement fusion in the laboratory, and its applications.

> **Philippe Baclet,** [a] **Claude Rullière,** [b] **Guy Schurtz** [c] and **Jacques Tassart** [d]
Military Applications Division
*(a) CEA/Valduc*
*(b) CEA/Aquitaine Scientific and Technical Research Center (CESTA)*
*(c) CEA/CESTA and CELIA (Intense Lasers and Applications Center – Mixed Research Unit CNRS-Université Bordeaux 1-CEA)*
*(d) CEA/DAM–Ile de France (DIF)*

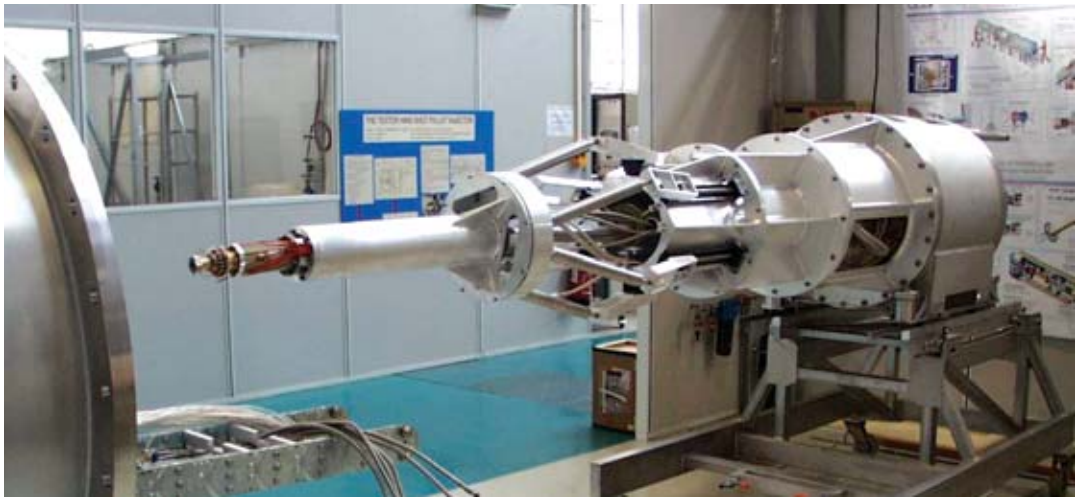

CEA

Illustration 8 :
Movable element of the cryogenic-target carrier undergoing design studies by CEA/DAM, in collaboration with the Low Temperatures Service (DSM/DRFMC) at Grenoble; its extremity receives the assembly shown in Figure 8b. The edge of the vacuum chamber may be seen in the foreground, at left.

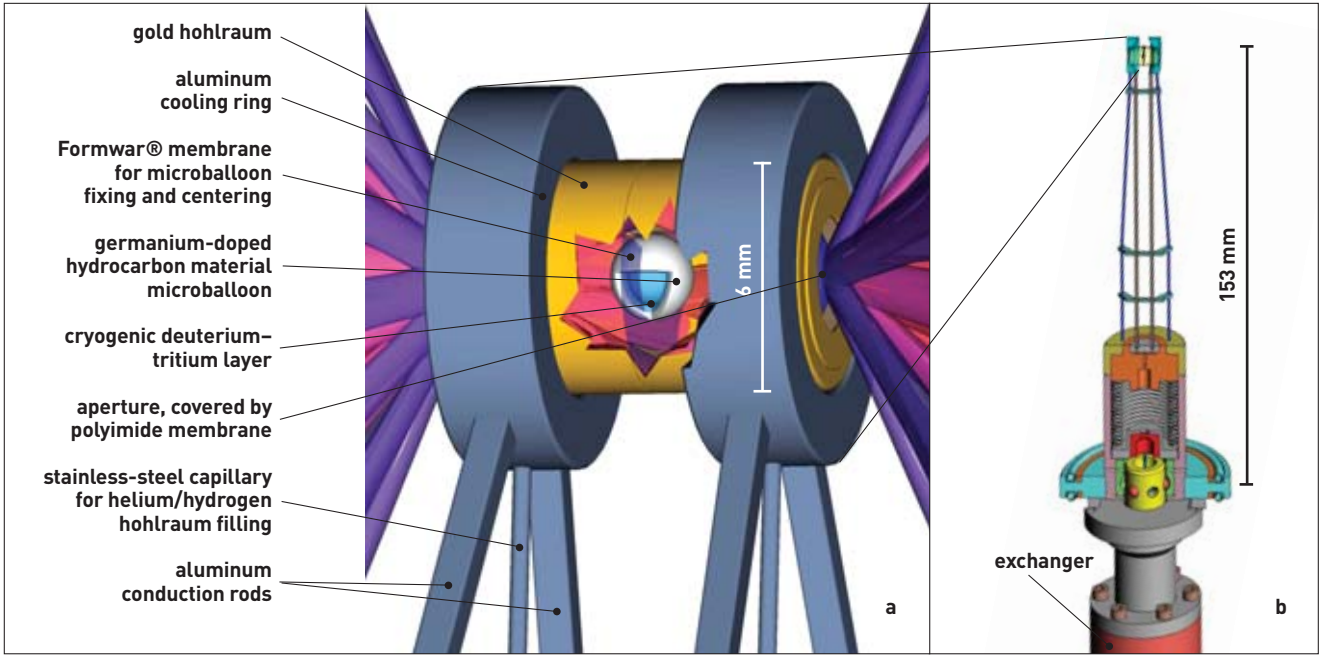


Figure 8.
Principle schematic of target functioning in indirect-drive inertial-confinement fusion. At (a), complete cryogenic hohlraum device; at (b), target assembly.